Contents lists available at ScienceDirect

Environmental Pollution

journal homepage: http://ees.elsevier.com

Size-dependent biochar breaking under compaction: Implications on clogging and pathogen removal in biofilters☆

Huong Le [a], Renan Valenca [a], Sujith Ravi [b], Michael Stenstrom [a], Sanjay Mohanty [a,*]

[a] Department of Civil and Environmental Engineering, University of California, Los Angeles, USA
[b] Department of Earth and Environmental Science, Temple University, Philadelphia, USA

ARTICLE INFO

Article history:
Received 23 May 2020
Received in revised form 2 July 2020
Accepted 5 July 2020
Available online xxx

Keywords
Stormwater treatment
Particle size
Disintegration
Fecal indicator bacteria
Hydraulic conductivity

ABSTRACT

Breaking of biochar during compaction of amended soil used in roadside biofilters or landfill cover can affect infiltration, clog amended soil, and change its pollutant removal capacity. It is unknown how the initial biochar size affects the biochar breaking, clogging potential, and contaminant removal capacity of biochar-amended soil. We compacted a mixture of coarse sand and biochar with sizes smaller than, similar to or larger than the sand and applied stormwater contaminated with *E. coli* in columns packed with the compacted sand-biochar mixture. Coating biochar with a dye and analyzing the dye concentration in the broken biochar particles eluted from the columns, we proved that biochar predominantly breaks under compaction by disintegration or splitting, not abrasion, and increases in biochar size decrease the likelihood of biochar breaking. We attribute this result to the effective dissipation of compaction energy through a greater number of contact points between a large biochar particle and the adjacent particles. Most of the broken biochar particles deposited in the pores, resulting in an exponential decrease in hydraulic conductivity of amended sand with an increase in suspended sediment loading. The clogging rate was higher in the columns with smaller biochar. The columns with small biochar also exhibited high *E. coli* removal capacity, partly because of an increase in straining by the smaller pore size created by the deposition of fine biochar particles created during compaction. These results are useful in selecting appropriate biochar size for its application in soils and roadside biofilters for water treatment.

1. Introduction

Road runoff conveys contaminants accumulated on impervious surfaces on roadways during dry weather and pollutes the receiving water bodies (Williamson and Water Quality Centre, 1993;Wang et al., 2001; Davis, 2005). Thus, the application of roadside stormwater treatment systems can treat road runoff, thereby potentially transforming the road infrastructures from being a source of water pollution into a mean for solution to water treatment and air quality (Shrestha et al., 2018; Shaneyfelt et al., 2017). Road banks are typically required to be compacted to 85–90% of its capacity to increase slope stability (California Department of Transportation, 2017); however, compaction limits infiltration or treatment of stormwater (Gregory et al., 2006; Batey and McKenzie, 2006). To increase infiltration in the compacted soils, bulking agents such as sand and gravel can be added, but they have limited potential to remove pollutants (Hatt et al., 2006). In this case, biochar can be added that has been shown to remove a wide range of pollutants (Boehm et al., 2020; Mohanty et al., 2018). Addition of biochar could not only increase infiltration in clay soil (Wong et al., 2018) with minimal effect on soil erosion (Kumar et al., 2019), but also improve treatment of organic contaminants (Lu and Chen, 2018), bacteria and heavy metals (Lau et al., 2017; Zhao et al., 2019; Sun et al., 2020). However, it is unclear how compaction affects biochar and its capacity to infiltrate and treat stormwater in biochar-augmented biofilters.

Under compaction, biochar particles could break by splitting or disintegration, and surface abrasion (Ghavanloughajar et al., 2020) because it has a lower load-bearing capacity than other soil amendments, including sand (Reza et al., 2012). The splitting of biochar particles can expose uncontaminated internal surfaces in the biochar for pollutant adsorption (Ding et al., 2018), whereas the abrasion of biochar can release biochar surface coating where pollutants may have been accumulated (Hameed et al., 2019). Although no study to date has examined how biochar properties may affect the breaking mechanism, it can be inferred from studies that used other porous media as listed in the review article (Yu, 2019). Particle shape and size under compaction could constrain particle breaking (Zhang and Baudet, 2013). For instance, smaller particles may slide into the pores between grains and result in abrasion of the particle surface, whereas large particles can be stuck near pores and split into pieces under compaction. On the other hand, the size of biochar particle may affect the number of con-

☆ This paper has been recommended for acceptance by Yong Sik Ok.
* Corresponding author.
E-mail address: mohanty@ucla.edu (S. Mohanty)

https://doi.org/10.1016/j.envpol.2020.115195
0269-7491/

tact points with neighbor particles through which compaction energy is dissipated, thereby affecting tensile stress at each contact point (McDowell and Bono, 2013). It is unclear which of the mechanisms is dominant for biochar, and more importantly, for biochar-sand mixtures under compaction.

Production and deposition of broken biochar particles can alter the flow path in compacted biofilters (Ghavanloughajar et al., 2020), which could lead to clogging of pores and change in contaminant removal. Compaction can increase the removal of bacteria in biofilters by increasing the contact time of stormwater in biofilter (Ghavanloughajar et al., 2020). As bacterial removal is sensitive to biochar size (Mohanty and Boehm, 2014; Sasidharan et al., 2016; Reddy et al., 2014), changes in biochar size due to breaking under compaction could affect bacterial removal. Compaction typically decreases the hydraulic conductivity of biofilters (Pitt et al., 2003). To reduce the negative impact of compaction, initial biochar size can be controlled as biochar size has been shown to affect the hydraulic conductivity of uncompacted sand or soil (Liu et al., 2016; Herath et al., 2013). However, these studies did not examine the clogging potential of biochar-amended biofilters. Biofilters can be clogged due to the accumulation of suspended sediments with a size predominantly smaller than 6 μm (Siriwardene et al., 2007) in the top of 20% of the filter media (Hatt et al., 2008). Although several studies have examined the design parameters to minimize clogging risk (Kandra et al., 2014; Le Coustumer et al., 2009), it is unclear how clogging rate is related to suspended sediment loading. Developing a model that predicts the clogging of compacted biofilters could help develop maintenance guidelines of roadside biofilters (Hatt et al., 2008; Le Coustumer and Barraud, 2007).

We aim to examine the effect of biochar size on the extent of biochar breaking under compaction, clogging rate, and *E. coli* removal in compacted biochar-sand filters. We hypothesize that the breaking of biochar particles would be sensitive to their initial size, which will also determine the clogging rate and *E. coli* removal in the compacted biofilters. To test the hypothesis, we packed mixtures of sand and biochar with different sizes under compaction in columns, applied contaminated stormwater, and compared the number of broken biochar particles released, the clogging rate, and *E. coli* removal. The results are helpful in developing design guidelines for biochar application in roadside biofilters.

2. Materials and methods

2.1. Stormwater preparation

Natural stormwater was collected from the Ballona Creek in Los Angeles, CA (34° 00′32″ N, 118° 23′3″ W), which receives dry-weather irrigation runoff from 318 km^2 urban area with 82% developed and 61% impervious surface. The detailed characteristics of stormwater was reported in the previous studies (Brown et al., 2013). Immediately after the collection, the stormwater was characterized for pH (Ion-Selective Electrode, model #9107BN, Fisher Scientific), conductivity (Two-Cell Accumet Probe, Fisher Scientific), and particle concentration, and stored at 4 °C until further use. To quantify initial particle release from biofilters after compaction, synthetic stormwater was used so that there were no particles in the influent. Synthetic stormwater was prepared by adding 10 mM NaCl to deionized (DI) water and adjusting the pH to 7.8 ± 0.2 using a small volume of concentrated HCl or NaOH. This step ensured that the ionic strength and pH, the geochemical driver for particle release or deposition, were consistent during particle release experiments.

Our preliminary study revealed that it would take years to clog the columns due to low concentration (< 30 mg L^{-1}) of suspended sediments in the natural stormwater. To accelerate the clogging during this study, turbid stormwater with a suspended solid concentration of 3 g L^{-1} was prepared by spiking fine (< 75 μm) sediments collected from a wetland that receives Ballona Creek stormwater (Valenca et al., 2020).

To examine removal of *E. coli*, the stormwater was spiked with kanamycin-resistant *E. coli* suspension following the method described elsewhere (Mohanty et al., 2014). Briefly, *E. coli* were cultured to a stationary phase, centrifuged and washed with phosphate buffer solution to remove the growth medium, and suspended in the collected stormwater to achieve an initial concentration of nearly 10^6 colony forming units (CFU) mL^{-1}.

2.2. Preparation of biofilter media

Commercially available biochar (Black Owl Biochar ™, Biochar Supreme, WA) and sand (20–30 Standard sand, Certified Material Testing Products, FL) were used. The coarse sand (0.6–0.85 mm) was washed in DI water to remove silica colloids and dried at 100 °C overnight. The biochar, produced by gasification of softwood at high temperature (900–1000 °C), was characterized for surface area, particle size distribution, elemental analysis, and ultimate and proximate analysis (Table S1). Biochar was sieved to remove particles smaller than 150 μm (mesh #100), to ensure fine particles released from biofilters were originated from the broken biochar produced during compaction. Biochar with a size greater than 2000 μm (mesh #10) was also removed to minimize preferential flow. The sieved biochar was further separated into three size fractions relative to the sand size: small (150 μm < d < 833 μm), medium (833 μm < d < 1180 μm), and large (1180 μm < d < 2000 μm). The sand was mixed with each biochar size fraction (5% biochar by weight) to prepare a homogeneous geomedia mixtures.

To examine the biochar breaking mechanisms under compaction, a portion of small and large biochar size fractions was coated with acridine orange dye (Fisher Scientific, MA) following the method described in the Supplementary Materials. The biochar-sand mixture was packed up to a 11.4-cm height (3 compacted layers) and subjected to stormwater infiltration to monitor release of broken biochar particles with different amounts of dye based on breaking mechanism.

2.3. Packing of filter media in model biofilter columns

Our previous study examined the effect of compaction conditions on biochar release by comparing the number of particles released from uncompacted and compacted columns (Ghavanloughajar et al., 2020). The current study examines the effect of biochar size on breaking mechanisms of biochar under compaction by comparing particle release in compacted columns with different biochar size fractions. A total of nine columns was packed in PVC columns (5.1 cm I.D. and 61.0 cm height), and triplicate columns were used for each of the media mixtures (Fig. S1). Before packing, a 9-cm drainage layer with pea gravels was created at the bottom of the column, and a nylon screen (100 μm pores) was placed on top of the gravel layer to prevent the biochar-sand mixture from falling into gravel layer. About 94–99 g of sand-biochar mixture was poured into the column and compacted to a height of a 3.8-cm using a Proctor hammer (2.5 kg). To ensure that comparable energy of a standard Proctor test was applied on the filter media, the Proctor hammer was dropped 7 times from 30.5-cm height per layer (more details in the Supporting materials). The procedure was repeated for 8 layers until the total filter media height reached 30.5 cm. An additional 2.5-cm layer of gravel was created on the top of the filter media to prevent the disturbance of biochar during stormwater application at the top of the filter media. The uniform packing of filter media was verified by measuring the bulk density for each layer (Fig. S2).

After packing, the columns were subjected to different test in the following order: (1) quantification of initial biochar particle release from compacted columns, (2) measurement of effective pore volume and flow-path heterogeneity by bromide tracer study, (3) estimation of *E. coli* removal capacity, and (4) quantification of clogging potential by measuring changes in hydraulic conductivity of the compacted biofilters with increases in suspended sediment loading. Separate columns were used to examine the breaking mechanism.

2.4. Release of biochar particles from compacted biofilters

To examine the initial release of biochar particles from the biofilters following compaction, 2 PV of synthetic stormwater (10 mM NaCl) was intermittently applied on the top of filter media at a flow rate of 8.5 mL min^{-1} using a peristaltic pump (Masterflex L/S Digital Drive, Cole Parmer). The flow rate was kept consistent to rule out the effect of flow fluctuation on particle release, as the increase in the flow is expected to increase particle mobilization (Shang et al., 2008). Effluents from the bottom of columns were collected at 0.5 PV fractions and analyzed for particle concentration and volume. The experiment was repeated every day for 5 consecutive days to examine if the quantity of particle released varied with successive rainfall events. Particle concentration was estimated based on the light (890 nm) absorbance of water samples (Ghavanloughajar et al., 2020).

2.5. Characterization of flow path heterogeneity in compacted biofilters

We conducted a bromide tracer study to estimate the effective pore volume of biofilters, which is corresponding to the volume of stormwater injected to achieve half of the highest bromide concentration in the inflow. Synthetic stormwater containing bromide (1 mM KBr) and 9 mM NaCl was applied at 8.5 mL min^{-1} on the top of each column for 1.2 h followed by application of bromide-free synthetic stormwater (10 mM NaCl) for 0.8 h to flush bromide solution from the pore water. The flow was interrupted, during which the bottom valve was closed, and the top of the column was sealed to prevent evaporation of stormwater. After 12 h of flow interruption, the flow was resumed for 0.5 h. The effluents were collected at 5–10 min intervals and analyzed for bromide using ion chromatography (Dionex™Integrion™ HPIC™ System, ThermoFisher). A change in bromide concentration during flow interruption was used as an indicator to qualitatively compare the extent of back-diffusion of solutes from immobile water trapped in compacted regions to bulk pore water in the flow paths (Brusseau et al., 1997).

2.6. E. coli removal in compacted biofilters

We chose *E. coli* to test the removal of particulate pollutants as their removal is more sensitive to change in pore size distribution under compaction than other dissolved pollutants. The *E. coli* removal capacity of compacted columns was tested following the method described in our previous study (Ghavanloughajar et al., 2020). Stormwater contaminated with *E. coli* at 10^6 CFU mL^{-1} was applied (8.5 mL m^{-1}) on the top of each column, and samples were collected at the bottom. The concentration of *E. coli* in the final 0.5 PV fraction, measured using an agar-plate technique, provides the steady-state removal capacity of the biofilter. It is expected that the *E. coli* concentration in the first flush would be lower due to adsorption or die-off of *E. coli* in the trapped pore water that contributes to first flush (Mohanty et al., 2014). The experiment was repeated for 5 consecutive days to determine if the bacterial removal capacity of compacted biofilters changes with an increase in exposure to contaminated stormwater.

2.7. Quantification of clogging potential of compacted biofilters

The hydraulic conductivity of each column was measured using a falling-head method (Supplementary materials). The clogging potential of each column was estimated by tracking the changes in hydraulic conductivity with increases in the loading of suspended sediments. The experiment was repeated until the hydraulic conductivity decreased to less than 1/10th of its initial value. The suspended sediment loading was estimated by multiplying the concentration of suspended sediments in the stormwater suspension with the cumulative volume of stormwater applied.

The deposition of suspended sediment is expected to decrease the effective porosity of filter media, which consequently affects their hydraulic conductivity. We used several models that have used the change in the filter media porosity to predict their hydraulic conductivity (Table S2). These models assume that the deposition of particles decreases the porosity of the column uniformly throughout the depths. Because clogging may occur by the formation of the cake layer without complete penetration of suspended sediments into the columns, we used an exponential empirical model (Phipps et al., 2007) that correlates hydraulic conductivity with sediment loading: $ln\left(K/K_0\right) = -rL$, where r is the sediment interaction coefficient related to properties of the filter media and sediments; L (kg/m^2) is the total sediment loading per unit coverage area of biofilter; $K_0$is the initial hydraulic conductivity before sediment loading; K is the final hydraulic conductivity of biofilter after sediment loading L.

2.8. Biochar breakage mechanism in biofilters during compaction

The small and large biochar size fractions were used to examine if the biochar breakage mechanism is sensitive to the initial biochar size. In the preliminary study and our previous study (Ghavanloughajar et al., 2020), we found that biochar with similar size to sand exhibited no specific trend in breaking mechanism and release compared with larger or smaller biochar, potentially due to limited contrast in number of contact point or changes in pore size distribution after packing. Thus, by analyzing only biochar smaller and larger than sand, we identify the breakage due to contrasting mechanisms. Separate columns were packed under compaction with previously dyed biochar (Supplementary Materials) and sand mixture following the same method outlined in Section 2.3. To examine the release of the broken biochar particles created during compaction, synthetic stormwater was slowly injected on the top of the packed columns, and effluent was collected to isolate and analyze the dye concentration on mobilized biochar particles. A small fraction of dyed biochar was analyzed to estimate the dye concentration of packed biochar before the mobilization experiment. The injection was repeated for 6 consecutive times. Particle concentration in the effluent was quantified following the method described elsewhere (Ghavanloughajar et al., 2020). Fluorescent intensity, an indicator for dye concentration on the biochar, of mobilized biochar particles, was measured after separating them from the stormwater to account for dissolved dye's fluorescence. 10 mL effluent was centrifuged at 4000 rpm for 15 min at room temperature, and the settled biochar particles were resuspended in 2 mL of DI water. Triplicated 100 μL sample from the processed suspension was added in 96-well plate, and dye intensity was measured within 30 min of sample collection to minimize dye decay during storage. The dye intensity was analyzed at excitation (460 nm) and emission (650 nm) of the dye using high-performance fluorescence equipment (GloMax Discover, Promega). Specific fluorescent intensity or normalized fluorescent intensity (FI) of mobilized biochar particles and packed biochar (similar to calibration standard) were compared to determine the biochar breaking mechanism.

To estimate the dye concentration on biochar in the packed biochar, 2.0 g of dyed biochar from the biochar pool used in the columns was manually ground for 10 min, suspended in 500 mL of DI water (more information under Supplementary Materials). The sample was diluted serially to measure an increase in dye concentration with an increase in biochar concentration (based on turbidity). The measured concentration provides a baseline dye concentration in the packed biochar. An increase or a decrease in the concentration of dye in mobilized biochar at the corresponding concentration of biochar in the suspension was assumed to be the result of biochar particle released from the surface or interior section of biochar, respectively. Such comparison permits the identification of biochar breaking mechanism: abrasion or fragmentation. Increase in dye concentration in the mobilized biochar relative to the bulk biochar is assumed to be because of abrasion, which releases biochar surface coating with a high concentration of dye, whereas a decrease in dye concentration in the mobilized biochar is assumed to be because of the splitting of biochar, which releases biochar particles from internal pores with low dye concentration.

2.9. Statistical analysis

One-way analysis of variance (ANOVA) was performed using R (version 3.6.1) between data sets to compare the parameters measured or estimated as a function of biochar particle size. The significance of differences (at $\alpha = 0.05$) between two specific means was assessed with the Tukey HSD post-hoc comparison test. Differences were considered significant at a *p*-value of less than 0.05.

3. Results

3.1. Quantity of particle released by the biofilter did not depend on biochar size

Infiltration of stormwater released fine biochar particles from biofilters, but the total quantity of particle released was independent of biochar size packed in the biofilters (Fig. 1). Although the concentration of particles released by medium and large biochar columns was initially high (>10 mg L^{-1}) due to the first-flush effect, the volume of the first sample was low compared to the total volume injected. Consequently, the total mass of biochar released initially has significant effect on the total cumulative mass of biochar released. Thus, the cumulative mass released by the columns were not statistically different ($p > 0.05$). The columns with large, medium and small biochar respectively released nearly 5.4 ± 2.3, 4.6 ± 1.3, and 4.4 ± 0.6 mg of fine biochar particles after 5 consecutive rainfall events. The amount released was negligible compared to the amount of biochar remained in the biofilters.

3.2. Stormwater interaction with compacted biochar was affected by biochar size

Biochar size in compacted biofilters affected the biofilter's pore volume, but this effect was more apparent in columns with small biochar particles (Fig. 2). The effective pore volume of the compacted biochar biofilters decreased with increases in biochar sizes (Fig. 2-B). Compaction is expected to create a low permeable zone, where diffusion of solute can become the dominant transport process. Flow interruption resulted in highest relative bromide concentration in the effluent of large biochar column, which confirms the presence of back diffusion of bromide from micropores in the low-permeable compacted zone to macropores. However, biochar size has no significant effect (p >

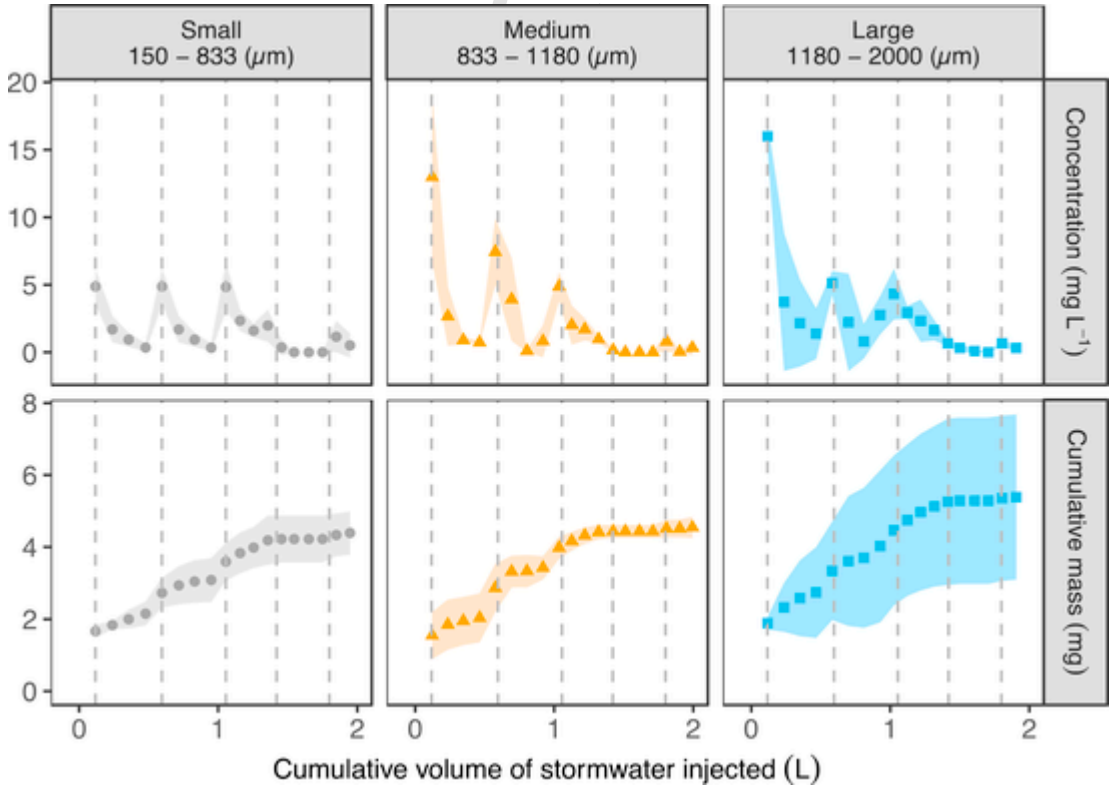

Fig. 1. Release of particles from compacted biochar-sand biofilters during intermittent infiltration of stormwater. Points represent mean value obtained from triplicated columns, and the shaded area represents one standard deviation over the mean.

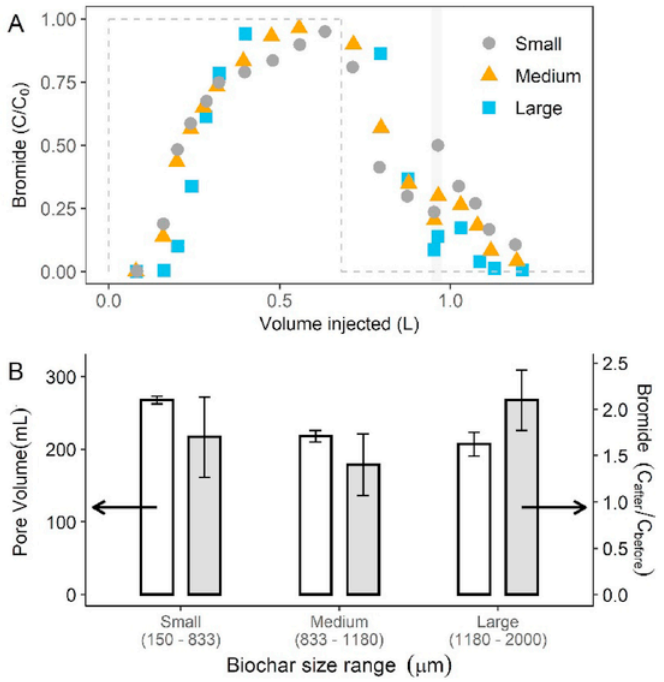

Fig. 2. (A) Breakthrough curves of bromide (a conservative tracer) in columns packed with compacted sand and biochar of three size ranges: small, medium and large biochar. The dashed line indicates the bromide concentration in the influent. Shaded vertical area indicates a flow interruption event. (B) White bar (left y-axis) indicates the effective pore volume of compacted columns, and grey filled bars (right y-axis) indicate the extent of bromide diffusion during flow interruption.

0.05) on the extent to which back diffusion of bromide occurred during flow interruption, indicating the amount of capillary pore space in internal pores of biochar particles or between particles did not change as a result of compaction. While compaction breaks particles and decrease capillary pore space in internal pores, compaction also creates smaller particles and provide additional capillary space between adjacent broken particles. Thus, the net effect is no significant change in the diffused region.

3.3. Removal of E. coli in compacted biofilters depended on initial biochar size

E. coli removal capacity of compacted biofilters with different biochar sizes was similar initially, but the removal capacity of biofilters with medium and large biochar decreased with increases in exposure to contaminated stormwater (Fig. 3). The removal in biofilters with small biochar particles mostly remained high: the effluent concentration was near detection limit.

3.4. Biochar size affected clogging potential of compacted biofilters

Initial hydraulic conductivity of compacted biofilters was the lowest for columns with small biochar, although the hydraulic conductivities of columns with medium and large biochar were not significantly different (***Fig. S3***). The hydraulic conductivity of all biofilters decreased with the increases in suspended sediment loading due to clogging (Fig. 4-A), but the clogging rate was the highest for biofilters with small biochar particles. Fitting the hydraulic conductivity with changes in porosity of biofilters using previous models listed in Table S2, we showed that porosity change because of the deposition of suspended sediments could not predict the clogging of biofilters (Fig. S4). The sediment interaction coefficient (r) increased with decreases in biochar size, particularly D_{10}—the diameter where 10% of the distribution has a smaller particle size (Fig. 4-B (insert)).

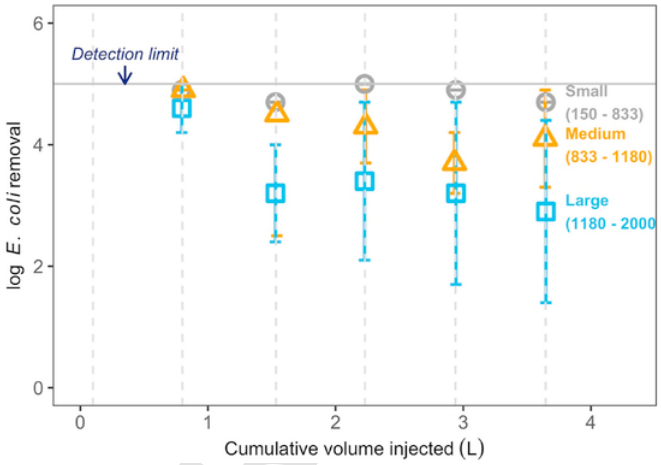

Fig. 3. Removal of *E. coli* during rainfall events. The error bars indicate one standard deviation over mean from triplicate columns with duplicate measurements per column (n = 6). The vertical dashed lines indicate the start of a rainfall event.

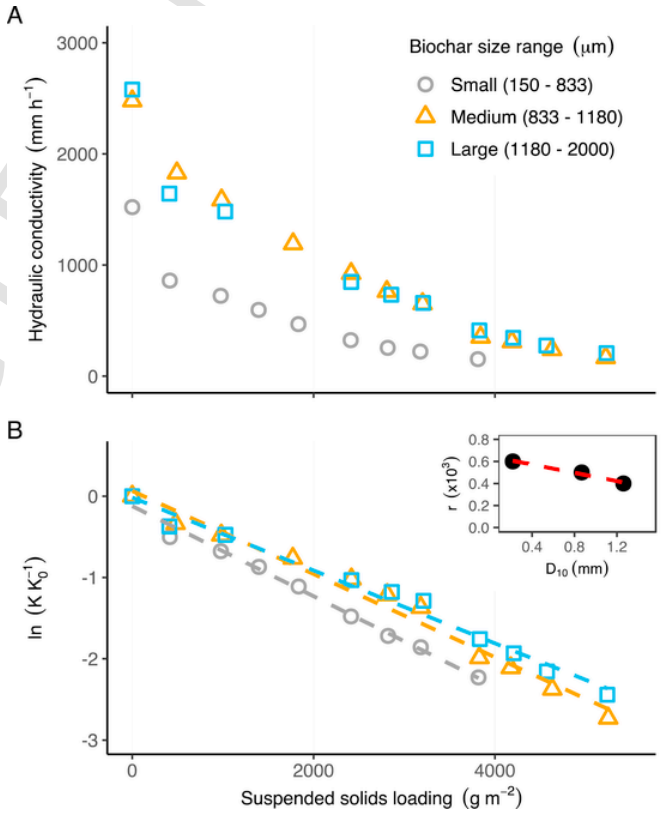

Fig. 4. (A) Suspended solid loading exponentially decreased the saturated hydraulic conductivity (K) of the compacted sand-biochar mixture. (B) Exponential model predicts relative changes in hydraulic rate (K/K0) with an increase in the suspended solid loading, with slopes (r) for columns with small, medium and large biochar were 0.0006, 0.0005 and 0.0004, respectively. $r = -0.0002\,D_{10} + 0.0006$. The insert in B shows the sediment interaction coefficient (r) increased with decreases in biochar size (D10).

3.5. Mechanism of biochar breaking during compaction depended on biochar size

We compared the specific fluorescent intensity of the mobilized biochar particles with that of the packed biochar as a function of the relative size of biochar to examine the relative importance of biochar breaking mechanisms—fragmentation vs. abrasion (Fig. 5). In

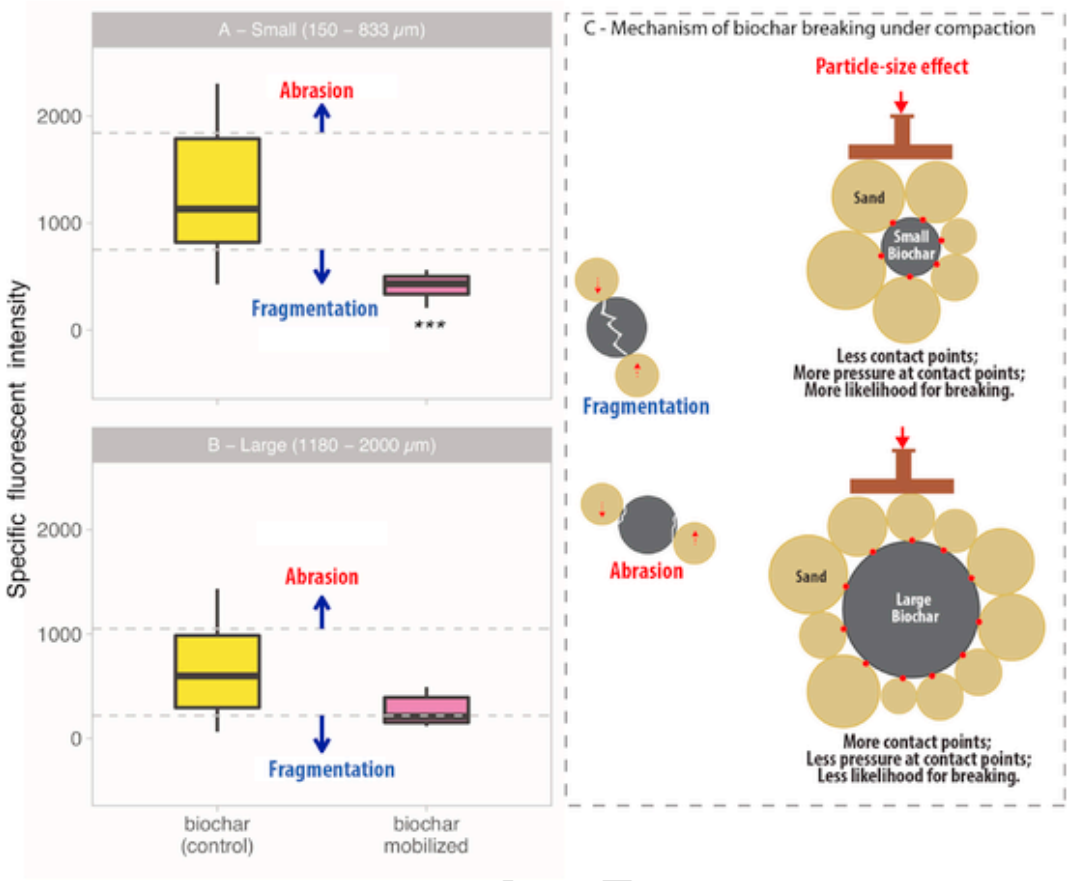

Fig. 5. Specific fluorescent intensity of packed biochar and mobilized biochar for (A) small biochar column and (B) large biochar column. *** indicates a p-value < 0.05. (C) The illustration shows the difference in compaction mechanisms (abrasion vs. fragmentation or splitting) and dissipation of compaction energy based on biochar size.

both columns, the specific fluorescent intensity of mobilized biochar was never more than that of packed biochar. A low dye concentration in mobilized biochar compared with packed column indicates abrasion is not the dominant biochar mechanism, and biochar predominantly breaks by fragmentation or splitting during compaction. In small biochar columns, the specific fluorescent intensity of mobilized biochar was significantly lower ($p < 0.05$) than that of packed biochar. In large biochar columns, the specific fluorescent intensity for both packed and mobilized biochar was not significantly different ($p > 0.05$). The result indicates that the extent of fragmentation depended on the relative size of biochar with sand.

4. Discussion

4.1. Biochar size effect on initial hydraulic conductivity and clogging potential

Columns with small biochar had the lowest initial hydraulic conductivity, although an increase in biochar size from medium to large did not significantly increase the hydraulic conductivity. In columns with medium and large biochar particles, sand is the dominant fraction and smaller than biochar. Thus, their hydraulic conductivity is dominated by sand size, which does not change as a result of compaction. In contrast, the columns with biochar smaller than the size of sand were significantly affected by compaction because compaction lowered the biochar particle size and potentially displaced them into the pores between sand particles. A decrease in pore space and blockage of flow paths can effectively decrease the hydraulic conductivity of the columns. The result supports the finding of previous studies (Liu et al., 2016; Trifunovic et al., 2018), where the decrease in the hydraulic conductivity following the addition of fine biochar particles was attributed to increased tortuosity and reduced porosity. A reduction in particle size of filter media is expected to decrease hydraulic conductivity (Liu et al., 2017) of filter media because of a reduction in pore size (Głąb et al., 2016). Nevertheless, these studies did not compact the filter media before examining their hydraulic conductivity. In our study, compaction coupled w + ith pore blockage by broken biochar particles produced during compaction synergistically lowered the hydraulic conductivity. The extent to which inter-particle pores can be filled with broken particles depended on the relative size of broken biochar particles with respect to pore size. As small biochar has small gap between particles, they are more susceptible to clogging. Our result confirmed this hypothesis.

The exponential empirical model predicted how fast a compacted column would clog based on the suspended sediment loading at the site. The result is similar to that observed by Wang et al. (2020), but their study did not account for the effect of compaction condition and filter media particle size. We showed that sediment interaction coefficient (r) increased with decreases in biochar size in the compacted biofilters. We also demonstrated that other traditional models (Table S2) that link saturated hydraulic conductivity with the porosity of filter media did not predict the changes in hydraulic conductivity with suspended sediment loading (Figs. S4 and S5). These models assume that the changes in porosity of biofilter should be uniform across the layers, which is unlikely in the stormwater biofilters. Compaction could particularly prevent penetration of suspended sediment beyond the top layer. The porosity of the top layer is expected to decrease rapidly compared to the rest of the filter media layers (Siriwardene et al., 2007; Hatt et al., 2008), and the change in the porosity in the top layer

could dictate the overall hydraulic conductivity of the biofilters. Therefore, a minor alteration in the column's overall porosity due to the deposition of suspended sediment resulted in a severe change in hydraulic conductivity. We provided empirical parameters linking particle size (D_{10}) with the clogging rate. The model enabled the use of the filter media size to predict the hydraulic conductivity of biofilters receiving runoff containing suspended sediments. The suspended sediment loading on a biofilter is a function of annual rainfall and characteristic of the catchment. Thus, the clogging rate in a biofilter can be estimated using the mean concentration of suspended sediments in stormwater, annual runoff volume passing through the biofilters, and particle size (D_{10}) of the biofilter media.

Hydraulic conductivity of biochar and sand mixture depends on the relative size of biochar compared with sand (Trifunovic et al., 2018); thus, the effect of compaction would depend on the changes in particle size of biochar. Our previous study (Ghavanloughajar et al., 2020) shows that the mean particle size of biochar-sand mixture decreases due to the breaking of biochar after compaction. We expect that the biochar would break in this study, but the changes in hydraulic conductivity would depend on the quantity of small biochar particles that can slide into the pores. Thus, biochar fragments larger than pore size would not affect hydraulic conductivity.

4.2. Mechanism of biochar breakage during compaction

The relative concentration of dye in mobilized biochar was significantly less than dye concentration on packed biochar. The result indicates that fragmentation by splitting, not abrasion, was the dominant mechanism of the breaking of small biochar particles under compaction. The fragmentation by splitting was less prominent for large biochar. Typically, abrasion occurs when particles slide against each other under compressive force. Biochar could slide into empty pores if the size of pores between sand or biochar particles was bigger than the sliding biochar. As a significant fraction of small biochar particles (150–833 μm) was still larger than the mean inter-particle pore size (373 μm) of sand (Trifunovic et al., 2018), abrasion was not found to be the dominant mechanism in our study. The lesser likelihood of "peeling" compared with "fracturing" during compaction suggests that compaction would expose new internal surface sites for contaminant adsorption, and the release of surface coating and any associate contaminants is less of a concern after compaction.

The fragmentation by splitting was less prominent for large biochar. We attributed the increased likelihood of biochar breaking by fragmentation in small biochar to a lower number of contact points between the biochar particle of interest and the adjacent particles that exert pressure on the biochar particle during compaction (Fig. 5). The contact points transmit compaction energy into the biochar particles; thus, lower number of contact points would result in higher tensile stress at each contact point (McDowell and Bono, 2013). As large biochar particles have a larger surface area than the small biochar particles, the numbers of contact points on large biochar particles would be greater than that of small biochar particles. Consequently, large biochar particles would experience less tensile stress at the points and be highly protected by numerous neighbors. In contrast, small particles could carry higher tensile stress at each contact point, leading to the formation of fractures through the biochar. This result is in agreement with the outcome of a previous study (Suescun-Florez et al., 2020) that showed that smaller sand particles break more than large sand particles. In summary, our result proved that the small particles are more likely to experience large tensile stress leading to their breaking under compaction primarily by fragmentation.

The mechanical properties of a biochar particle are dependent on temperature and residence time during pyrolysis, not particle size (Das et al., 2015). However, mechanical properties of bulk biochar and sand mixture may vary with particle size based on dissipation of compaction force due to either displacement of biochar particles into the pore space or breaking of biochar particles. Direct evidence using an optical microscope is not feasible because biochar and sand are opaque, and possible disturbance of biochar and sand grains during compaction and during sample preparation for optical imaging (See Supporting material, Fig. S6). Future studies should use a transparent column packed with transparent glass beads and biochar to observe the breaking mechanism under compaction.

4.3. Release of fine particles after compaction was independent of biochar size

We found that the particle size of biochar in the compacted biofilter did not affect the net particle released from the filter media. About 5 mg of fine biochar particles were released, which is less than 0.1% of biochar remained in the column, indicating the majority of biochar particles created during compaction are retained in the column irrespective of the size of biochar particles before compaction. The particle released from compacted biofilters is a function of the total particle pool created during compaction due to the breaking of biochar, and the fraction of the generated particle pool available for transport based on the width of the pore path or hydraulic conductivity (Ghavanloughajar et al., 2020). Although the columns with large biochar had higher initial hydraulic conductivity (or high transport potential of broken particles), the pool of broken particles created during compaction could be low because of their limited fragmentation, as explained earlier. Similarly, the columns with small biochar would have a larger pool of broken particles created by fragmentation during compaction, but most of them could be trapped in the columns due to low hydraulic conductivity (or low transport potential). As the biochar size in the filter media had the opposite effect on the generation of biochar particles during compaction, and their transportation after compaction, the net amount of biochar particles mobilized became independent of biochar size in the filter media.

4.4. E. coli removal capacity of compacted biofilters was sensitive to biochar size

E. coli removal capacity of compacted biofilters decreased with increases in exposure to contaminated stormwater only if the biochar size was similar or greater than the size of sand. The removal remained consistently high in biofilters packed with biochar smaller than the size of sand, indicating an increase in overall surface sites by breaking of biochar particles lowered the exhaustion rate of biochar adsorption capacity. Previous studies showed that eliminating fine particles decreased the removal capacity of biochar-augmented biofilters (Mohanty and Boehm, 2014; Sasidharan et al., 2016; Reddy et al., 2014). Hence, creation of fine particles by compaction is expected to increase bacteria removal. Our results show that smaller biochar is more likely to break under compaction, thereby exposing more surfaces for adsorption. The biochar fragments can clog the pore paths and increase the removal of bacteria by straining (Sasidharan et al., 2016). However, mobilization of fine biochar carrying *E. coli* from biofilters due to disturbance during compaction could increase the *E. coli* concentration in the effluent (Mohanty and Boehm, 2015). However, our study shows that the initial release of biochar particles is insignificant, and they are irrelevant after the initial first flush. Thus, initial biochar particle size should be selected to optimize the effect of compaction on both infiltration and *E. coli* removal in biofilters.

5. Conclusions

The results revealed the importance of biochar size on their breaking by compaction, clogging rate, and bacterial removal in com-

pacted biofilters. The main conclusions are:

- Under compaction, biochar predominantly broke by fragmentation, not abrasion. The initial loss of biochar particles with infiltrating water was negligible, indicating the broken biochar particles were trapped in the packed columns.
- The hydraulic conductivity of compacted biochar columns exponentially decreased with increases in suspended sediment loading. The clogging rate was higher in the columns with small biochar. The empirical model based on suspended sediment loading and particle size (D_{10}) of packed media could predict the clogging rate compacted biochar-amended sand.
- The change in *E. coli* removal with an increase in stormwater loading was sensitive to biochar size in the compacted columns. The removal capacity of columns packed with biochar smaller than sand was consistently high, whereas the removal capacity of columns packed with biochar with the size same or larger than sand decreased with an increase in stormwater loading.
- The results showed that the use of large-sized biochar can minimize the negative impact of compaction on infiltration capacity or clogging of biofilters, but their capacity to remove *E. coli* may decrease with time. Thus, the size of biochar should be optimized to limit clogging and increase pathogen removal.

CRediT authorship contribution statement

Huong Le: Writing - original draft. **Renan Valenca:** Visualization, Formal analysis. **Sujith Ravi:** Writing - review & editing. **Michael Stenstrom:** Writing - review & editing. **Sanjay Mohanty:** Conceptualization, Funding acquisition, Writing - original draft, Writing - review & editing.

Declaration of competing interest

The authors declare that they have no known competing financial interests or personal relationships that could have appeared to influence the work reported in this paper.

Acknowledgments

We acknowledge the generous contribution donation of biochar from Biochar Supreme Co (Everson, WA). The work is partially supported by the California Department of Transportation (Caltrans). The views expressed in this document are solely those of the authors and do not necessarily reflect those of the agency. Caltrans does not endorse any products mentioned in this publication.

Appendix A. Supplementary data

Supplementary data to this article can be found online at https://doi.org/10.1016/j.envpol.2020.115195.

References

Batey, T, McKenzie, D C, 2006. Soil compaction: identification directly in the field. Soil Use Manag. 22 (2), 123–131. doi:10.1111/j.1475-2743.2006.00017.x.

Boehm, A B, Bell, C D, Fitzgerald, N J M, Gallo, E, Higgins, C P, Hogue, T S, Luthy, R G, Portmann, A C, Ulrich, B A, Wolfand, J M, 2020. Biochar-augmented biofilters to improve pollutant removal from stormwater – can they improve receiving water quality? Environ. Sci. Water Res. Technol.. doi:10.1039/D0EW00027B.

Brown, J S, Stein, E D, Ackerman, D, Dorsey, J H, Lyon, J, Carter, P M, 2013. Metals and bacteria partitioning to various size particles in Ballona creek storm water runoff. Environ. Toxicol. Chem. 32 (2), 320–328. doi:10.1002/etc.2065.

Brusseau, M L, Hu, Q, Srivastava, R, 1997. Using flow interruption to identify factors causing nonideal contaminant transport. J. Contam. Hydrol. 24 (3), 205–219 https://doi.org/10.1016/S0169-7722(96)00009-5.

California Department of Transportation, 2017. Highway Design Manual Sixth Edition. Retrieved from. https://dot.ca.gov/-/media/dot-media/programs/design/documents/hdm-complete-14dec2018.pdf.

Das, O, Sarmah, A K, Bhattacharyya, D, 2015. Structure–mechanics property relationship of waste derived biochars. Sci. Total Environ. 538, 611–620. doi:10.1016/j.scitotenv.2015.08.073.

Davis, A P, 2005. Green engineering principles promote low-impact development. Environ. Sci. Technol. 39 (16), 338A–344A. doi:10.1021/es053327e.

Ding, L, Tan, W, Xie, S, Mumford, K, Lv, J, Wang, H, Fang, Q, Zhang, X, Wu, X, Li, M, 2018. Uranium adsorption and subsequent re-oxidation under aerobic conditions by Leifsonia sp. - coated biochar as green trapping agent. Environ. Pollut. 242, 778–787. doi:10.1016/j.envpol.2018.07.050.

Ghavanloughajar, M, Valenca, R, Le, H, Rahman, M, Borthakur, A, Ravi, S, Stenstrom, M K, Mohanty, S, 2020. Compaction conditions affect the capacity of biochar-amended sand filters to treat road runoff. Sci. Total Environ. 139180. doi:10.1016/j.scitotenv.2020.139180.

Głąb, T, Palmowska, J, Zaleski, T, Gondek, K, 2016. Effect of biochar application on soil hydrological properties and physical quality of sandy soil. Geoderma 281, 11–20. doi:10.1016/j.geoderma.2016.06.028.

Gregory, J H, Dukes, M D, Jones, P H, Miller, G L, 2006. Effect of urban soil compaction on infiltration rate. J. Soil Water Conserv. 61 (3), 117–124. https://www.jswconline.org/content/61/3/117.

Hameed, R, Cheng, L, Yang, K, Fang, J, Lin, D, 2019. Endogenous release of metals with dissolved organic carbon from biochar: effects of pyrolysis temperature, particle size, and solution chemistry. Environ. Pollut. 255 (113253). doi:10.1016/j.envpol.2019.113253.

Hatt, B E, Siriwardene, N, Deletic, A, Fletcher, T D, 2006. Filter media for stormwater treatment and recycling: the influence of hydraulic properties of flow on pollutant removal. Water Sci. Technol. 54 (6–7), 263–271. doi:10.2166/wst.2006.626.

Hatt, Belinda E, Fletcher, T D, Deletic, A, 2008. Hydraulic and pollutant removal performance of fine media stormwater filtration systems. Environ. Sci. Technol. 42 (7), 2535–2541. doi:10.1021/es071264p.

Herath, H M S K, Camps-Arbestain, M, Hedley, M, 2013. Effect of biochar on soil physical properties in two contrasting soils: an Alfisol and an Andisol. Geoderma 209–210, 188–197. doi:10.1016/j.geoderma.2013.06.016.

Kandra, Harpreet Singh, Deletic, A, McCarthy, D, 2014. Assessment of impact of filter design variables on clogging in stormwater filters. Water Resour. Manag. 28 (7), 1873–1885. doi:10.1007/s11269-014-0573-7.

Kumar, H, Ganesan, S P, Bordoloi, S, Sreedeep, S, Lin, P, Mei, G, Garg, A, Sarmah, A K, 2019. Erodibility assessment of compacted biochar amended soil for geo-environmental applications. Sci. Total Environ. 672, 698–707. doi:10.1016/j.scitotenv.2019.03.417.

Lau, A Y T, Tsang, D C W, Graham, N J D, Ok, Y S, Yang, X, Li, X, 2017. Surface-modified biochar in a bioretention system for Escherichia coli removal from stormwater. Chemosphere 169, 89–98. doi:10.1016/j.chemosphere.2016.11.048.

Le Coustumer, S, Barraud, S, 2007. Long-term hydraulic and pollution retention performance of infiltration systems. Water Sci. Technol. 55 (4), 235–243 https://doi.org/10.2166/wst.2007.114.

Le Coustumer, Sébastien, Fletcher, T D, Deletic, A, Barraud, S, Lewis, J F, 2009. Hydraulic performance of biofilter systems for stormwater management: Influences of design and operation. J. Hydrol. 376 (1), 16–23. doi:10.1016/j.jhydrol.2009.07.012.

Liu, Z, Dugan, B, Masiello, C A, Barnes, R T, Gallagher, M E, Gonnermann, H, 2016. Impacts of biochar concentration and particle size on hydraulic conductivity and DOC leaching of biochar– sand mixtures. J. Hydrol. 533, 461–472. doi:10.1016/j.jhydrol.2015.12.007.

Liu, Z, Dugan, B, Masiello, C A, Gonnermann, H M, 2017. Biochar particle size, shape, and porosity act together to influence soil water properties. PloS One 12 (6), e0179079 https://doi.org/10.1371/journal.pone.0179079.

Lu, L, Chen, B, 2018. Enhanced bisphenol A removal from stormwater in biochar-amended biofilters: combined with batch sorption and fixed-bed column studies. Environ. Pollut. 243, 1539–1549. doi:10.1016/j.envpol.2018.09.097.

McDowell, G R, de Bono, J P, 2013. On the micro mechanics of one-dimensional normal compression. Geotechnique 63 (11). https://doi:10.1680/geot.12.P.041.

Mohanty, S K, Boehm, A B, 2014. Escherichia coli removal in biochar-augmented biofilter: effect of infiltration rate, initial bacterial concentration, biochar particle size, and presence of compost. Environ. Sci. Technol. 48 (19), 11535–11542. doi:10.1021/es5033162.

Mohanty, S K, Boehm, A B, 2015. Effect of weathering on mobilization of biochar particles and bacterial removal in a stormwater biofilter. Water Res. 85, 208–215. doi:10.1016/j.watres.2015.08.026.

Mohanty, S K, Cantrell, K B, Nelson, K L, Boehm, A B, 2014. Efficacy of biochar to remove Escherichia coli from stormwater under steady and intermittent flow. Water Res. 61, 288–296. doi:10.1016/j.watres.2014.05.026.

Mohanty, S K, Valenca, R, Berger, A W, Yu, I K M, Xiong, X, Saunders, T M, Tsang, D C W, 2018. Plenty of room for carbon on the ground: potential applications of biochar for stormwater treatment. Sci. Total Environ. 625, 1644–1658 https://doi.org/10.1016/j.scitotenv.2018.01.037.

Phipps, D W, Jr., Lyon, S, Hutchinson, A S, 2007. Development of a percolation decay model to guide future optimization of surface water recharge basins. In: Fox, P (Ed.), Management of Aquifer Recharge for Sustainability, Proceedings of 6th International Symposium on Managed Aquifer Recharge of Groundwater. Acacia Publishing, Phoenix, pp. 433–466.

Pitt, R E, Chen, S-E, Clark, S, Lantrip, J, Ong, C K, Voorhees, J, 2003. Infiltration through compacted urban soils and effects on Biofiltration design. J. Water Manag. Model.. doi:10.14796/JWMM.R215-12.

Reddy Krishna, R, Tao, Xie, Sara, Dastgheibi, 2014. Evaluation of biochar as a potential filter media for the removal of mixed contaminants from urban storm water runoff. J. Environ. Eng. 140 (12), 04014043 https://doi.org/10.1061/(ASCE)EE.1943-7870.0000872.

Reza, M T, Lynam, J G, Vasquez, V R, Coronella, C J, 2012. Pelletization of biochar from hydrothermally carbonized wood. Environ. Prog. Sustain. Energy 31 (2), 225–234. doi:10.1002/ep.11615.

Sasidharan, S, Torkzaban, S, Bradford, S A, Kookana, R, Page, D, Cook, P G, 2016. Transport and retention of bacteria and viruses in biochar-amended sand. Sci. Total Environ. 548–549, 100–109. doi:10.1016/j.scitotenv.2015.12.126.

Shaneyfelt, K M, Anderson, A R, Kumar, P, Hunt, W F, 2017. Air quality considerations for stormwater green street design. Environ. Pollut. 231, 768–778. doi:10.1016/j.envpol.2017.08.081.

Shang, J, Flury, M, Chen, G, Zhuang, J, 2008. Impact of flow rate, water content, and capillary forces on in situ colloid mobilization during infiltration in unsaturated sediments. Water Resour. Res. 44 (6). doi:10.1029/2007WR006516.

Shrestha, P, Hurley, S E, Wemple, B C, 2018. Effects of different soil media, vegetation, and hydrologic treatments on nutrient and sediment removal in roadside bioretention systems. Ecol. Eng. 112, 116–131. doi:10.1016/j.ecoleng.2017.12.004.

Siriwardene, N R, Deletic, A, Fletcher, T D, 2007. Clogging of stormwater gravel infiltration systems and filters: Insights from a laboratory study. Water Res. 41 (7), 1433–1440. doi:10.1016/j.watres.2006.12.040.

Suescun-Florez, E, Iskander, M, Bless, S, 2020. Evolution of particle damage of sand during axial compression via arrested tests. Acta Geotechnica 15 (1), 95–112 https://doi.org/10.1007/s11440-019-00892-w.

Sun, Y, Chen, S S, Lau, A Y T, Tsang, D C W, Mohanty, S K, Bhatnagar, A, Rinklebe, J, Lin, K-Y A, Ok, Y S, 2020. Waste-derived compost and biochar amendments for stormwater treatment in bioretention column: Co-transport of metals and colloids. J. Hazard Mater. 383 (121243). doi:10.1016/j.jhazmat.2019.121243.

Trifunovic, B, Gonzales, H B, Ravi, S, Sharratt, B S, Mohanty, S K, 2018. Dynamic effects of biochar concentration and particle size on hydraulic properties of sand. Land Degrad. Dev. 29 (4), 884–893. doi:10.1002/ldr.2906.

Valenca, R, Ramnath, K, Dittrich, T M, Taylor, R E, Mohanty, S K, 2020. Microbial quality of surface water and subsurface soil after wildfire. Water Res. 175 (115672) https://doi.org/10.1016/j.watres.2020.115672.

Wang, L, Lyon, J, Kanehl, P, Bannerman, R, 2001. Impacts of urbanization on stream habitat and fish across multiple spatial scales. Environ. Manag. 28 (2), 255–266. doi:10.1007/s0026702409.

Wang, H, Xin, J, Zheng, X, Li, M, Fang, Y, Zheng, T, 2020. Clogging evolution in porous media under the coexistence of suspended particles and bacteria: Insights into the mechanisms and implications for groundwater recharge. J. Hydrol. 582 (124554) https://doi.org/10.1016/j.jhydrol.2020.124554.

Williamson, R B, Water Quality Centre, 1993. Urban runoff data book: a manual for the preliminary evaluation of urban stormwater impacts on water quality. In: Hamilton, N Z (Ed.), Water Quality Centre, Ecosystems Division, National Institute of Water and Atmospheric Research, second ed. https://trove.nla.gov.au/version/12761345.

Wong, J T F, Chen, Z, Wong, A Y Y, Ng, C W W, Wong, M H, 2018. Effects of biochar on hydraulic conductivity of compacted kaolin clay. Environ. Pollut. 234, 468–472. doi:10.1016/j.envpol.2017.11.079.

Yu, F, 2019. Particle breakage in granular soils: a review. Part. Sci. Technol. 1–10. doi:10.1080/02726351.2019.1666946.

Zhang, X, Baudet, B A, 2013. Particle breakage in gap-graded soil. Géotechnique Lett. 3 (2), 72–77. doi:10.1680/geolett.13.00022.